Inorganic Chemistry
Article

Inorg. Chem. **2010**, *49*, 5101–5106 **5101**
DOI: 10.1021/ic1002572

A Quantum Mechanical Charge Field Molecular Dynamics Study of Fe^{2+} and Fe^{3+} Ions in Aqueous Solutions

Syed Tarique Moin, Thomas S. Hofer, Andreas B. Pribil, Bernhard R. Randolf, and Bernd M. Rode*

*Theoretical Chemistry Division, Institute of General, Inorganic and Theoretical Chemistry,
University of Innsbruck, Innrain 52a, A-6020 Innsbruck, Austria*

Received February 8, 2010

Ab initio quantum mechanical charge field molecular dynamics (QMCF-MD) simulations have been performed for aqueous solutions of Fe^{2+} and Fe^{3+} ions at the Hartree−Fock level of theory to describe and compare their structural and dynamical behavior. The structural features of both hydrated ions are characterized by radial distribution functions that give the maximum probability of the ion−O distance for Fe^{2+} and Fe^{3+} ions at 2.15 and 2.03 Å, respectively. The angular distribution functions of both ions prove the octahedral arrangement of six water ligands, whereas the second shells of these ions differ. Both ions show influence on the water molecules beyond the second shells. The structure-forming abilities of both ions are visible from the ligand mean residence times and ion−O stretching frequencies evaluated for both ions. The substantially improved data obtained from these QMCF-MD simulations show better correlation with available experimental results than the conventional quantum mechanics/molecular mechanics molecular dynamics (QM/MM MD) approaches with one hydration shell treated by quantum mechanics.

1. Introduction

Iron is involved in numerous biological[1−3] and chemical processes,[4,5] in the form of either metal or ferrous (Fe^{2+}) and ferric (Fe^{3+}) ions. The hydration structures of these ions have been the subject of many experimental[6−9] and theoretical studies.[10−12] Earlier theoretical studies of Fe^{2+} and Fe^{3+} ions in water were based on effective pair potentials,[10] potentials based on the polarizable continuum model for the solvent[11] and on the quantum mechanics/molecular mechanics molecular dynamics (QM/MM MD) approach[13] using the concept that the chemically most relevant region utilizes quantum mechanics while the rest of the system is described by ab initio derived potentials. Those simulation studies of Fe^{2+} and Fe^{3+} ions in aqueous solutions had been performed to evaluate the solvation shell structure,[10−12,14−,16] hydrolysis,[17] charge-transfer reactions,[18,19] and others.[20,21] Car−Parinello molecular dynamics simulations were also performed on the Fe^{2+} and Fe^{3+} ions in solution[22−24] using the BLYP functional and limiting the number of ligands to 30−60 molecules. Previous ab initio QM/MM MD[13] simulations for Fe^{2+}(aq) and Fe^{3+}(aq) ions were performed for the ions and only one hydration shell in the QM region, and because of the data for other hydrated ions,[25,26] this could have caused some

---

*To whom correspondence should be addressed. E-mail: Bernd.M.Rode@uibk.ac.at. Tel.: +43-512-507-5129. Fax: +43-512-507-2714.

(1) Brar, S.; Henderson, D.; Schenck, J.; Zimmerman, E. A. *Arch. Neurol.* **2009**, *66*(3), 371.
(2) Nanami, M.; Ookawara, T.; Otaki, Y.; Ito, K.; Moriguchi, R.; Miyagawa, K.; Hasuike, Y.; Izumi, M.; Eguchi, H.; Suzuki, K.; Nakanishi, T. *Arterioscler., Thromb., Vasc. Biol.* **2005**, *25*(12), 2495.
(3) Glei, M.; Klenow, S.; Sauer, J.; Wegewitz, U.; Richter, K.; Pool-Zobel, B. L. *Mutat. Res.* **2006**, *594*(1), 162.
(4) Enthaler, S.; Junge, K.; Beller, M. *Angew. Chem., Int. Ed.* **2008**, *47*, 3317.
(5) Fox, B. A.; Threlfall, T. L. *Org. Synth.* **1973**, *5*, 346.
(6) Ohtaki, H.; Radnai, T. *Chem. Rev.* **1993**, *93*, 1157.
(7) Neilson, G. W.; Enderby, J. E. *Adv. Inorg. Chem.* **1989**, *34*, 196.
(8) Herdman, G. J.; Neilson, G. W. *J. Phys.: Condens. Matter* **1992**, *4*, 649.
(9) Herdman, G. J.; Neilson, G. W. *J. Phys.: Condens. Matter* **1992**, *4*, 627.
(10) Curtiss, L. A.; Halley, J. W.; Hautman, J.; Rahman, A. *J. Chem. Phys.* **1987**, *86*, 2319.
(11) Floris, F.; Persico, M.; Tani, A.; Tomasi, J. *Chem. Phys. Lett.* **1992**, *199*(6), 518.
(12) Dégrève, L.; Quintale, C. *J. Electroanal. Chem.* **1996**, *409*(1), 25.
(13) Remsungnen, T.; Rode, B. M. *J. Phys. Chem. A* **2003**, *107*(13), 2324.
(14) Kneifel, C. L.; Friedman, H. L.; Newton, M. D. *Z. Naturforsch. A* **1989**, *44*(5), 385.
(15) Kneifel, C. L.; Friedman, H. L.; Newton, M. D. *J. Mol. Liq.* **1994**, *66* (1), 107.
(16) Guárdia, E.; Padró, J. A. *Chem. Phys.* **1990**, *144*(3), 353.
(17) Rustad, J. R.; Hay, B. P.; Halley, J. W. *J. Chem. Phys.* **1995**, *102*(3), 427.
(18) Kuharski, R. A.; Bader, J. S.; Chandler, D.; Sprik, M.; Klein, M. L.; Impey, R. W. *J. Chem. Phys.* **1988**, *89*(5), 3248.
(19) González-Lafont, A.; Lluch, J. M.; Oliva, A.; Bertrán, J. *J. Comput. Chem.* **2004**, *12*(10), 1165.
(20) Bader, J. S.; Chandler, D. *J. Phys. Chem.* **1992**, *96*(15), 6423.
(21) Kumar, P. V.; Tembe, B. L. *J. Chem. Phys.* **1992**, *97*(6), 4356.
(22) Ensing, B.; Baerends, E. J. *J. Phys. Chem. A* **2002**, *106*(34), 7902.
(23) Ensing, B.; Buda, F.; Blöchl, P. E.; Baerends, E. J. *Phys. Chem. Chem. Phys.* **2002**, *4*(15), 3619.
(24) Amira, S.; Spangberg, D.; Zelin, V.; Probst, M.; Hermansson, K. *J. Phys. Chem. B* **2005**, *109*(29), 14235.
(25) DIncal, A.; Hofer, T. S.; Randolf, B. R.; Rode, B. M. *Phys. Chem. Chem. Phys.* **2006**, *8*, 2841.
(26) Kritayakornupong, C.; Plankensteiner, K.; Rode, B. M. *J. Comput. Chem.* **2004**, *25*(13), 1576.

Table 1. Average Binding Energies for the $[Fe(H_2O)_n]^{2+}$ and $[Fe(H_2O)_n]^{3+}$ Complexes, Obtained from HF, CCSD, MP2, and B3LYP Calculations

n	HF	CCSD	MP2	B3LYP
		$[Fe(H_2O)_n]^{2+}$		
2	−75.93	−83.37	−83.81	−94.64
4	−67.04		−72.30	−76.94
6	−57.87		−61.70	−63.90
		$[Fe(H_2O)_n]^{3+}$		
2	−151.05	−164.19	−163.56	−192.03
4	−128.37		−135.98	−149.68
6	−109.37		−114.54	−122.15

Table 2. Average Fe^{2+}−O and Fe^{3+}−O Distances (Å) for $[Fe(H_2O)_n]^{2+}$ and $[Fe(H_2O)_n]^{3+}$ Complexes, Obtained from HF, CCSD, MP2, and B3LYP Calculations

n	HF	CCSD	MP2	B3LYP
		$r_{Fe^{2+}-O}$		
2	2.00	1.96	1.96	1.94
4	2.09		2.06	2.04
6	2.20		2.16	2.15
		$r_{Fe^{3+}-O}$		
2	1.89	1.88	1.87	1.92
4	1.97		1.95	1.95
6	2.06		2.04	2.05

errors. Hence, we performed quantum mechanical charge field molecular dynamics (QMCF-MD) simulations for Fe^{2+} and Fe^{3+} ions, which included both first and second hydration shells fully into the QM region and provided a number of other improvements in the evaluation of forces.[27]

2. Methods

Simulation Methods. For the QMCF-MD simulations, suitable basis sets for these aqueous ionic (Fe^{2+} and Fe^{3+}) systems were selected on the basis of the structural properties reproduced compared to the geometry optimization calculations performed with larger basis set by Remsungnen et al.[13,28,29] for $[Fe(H_2O)_{n=2,4,6}]^{2+}$ and $[Fe(H_2O)_{n=2,4,6}]^{3+}$ complexes. Ab initio unrestricted geometry optimizations were performed by employing the SBKJC-VDZ-ECP[30−33] basis set for Fe and Dunning double-ζ plus polarization[34,35] basis sets for H and O atoms of water molecules at different levels of theory. Table 1 shows the calculated binding energies per ligand for these complexes from optimized configurations. The Hartree−Fock (HF) values are lower than those of correlated methods, but the B3LYP values are by a larger extent too high, which would inevitably lead to too rigid structures. This trend is even more pronounced in the case of $[Fe(H_2O)_{n=2,4,6}]^{3+}$ complexes than in $[Fe(H_2O)_{n=2,4,6}]^{2+}$ complexes. However, the ion−O distances for these ion−water clusters (cf. Table 2) at the HF level deviate more from the correlated methods (MP2 and CCSD) than those of B3LYP, which are in most cases slightly too short. The thermochemical data and partly also the structural characteristics reaffirm the limited capability of density functional theory methods for the description of water[36] and aqueous solutions.[25] The HF level of theory could be considered, therefore, as the most appropriate computationally affordable compromise between accuracy and cost.

The ab initio QMCF-MD methodology[27] has worked very well with a variety of solutes such as metal complexes and composite anions[37,38] without the need for constructing any potential functions except that for solvent−solvent interactions. The QMCF-MD approach utilizes a partitioning scheme in which the system is divided into three regions: the core region with the metal ion and its first hydration shell, the layer region containing the second hydration shell, which both are treated quantum mechanically, and the MM region, where the particles are taken into account by force-field potentials. The incorporation of point charges assigned to atoms in the MM region that dynamically change their positions in the core Hamiltonian for the QM region via a perturbation term is also one of the advantages of the QMCF-MD methodology.

$$V' = \sum_{J=1}^{M} \frac{q_J}{r_{iJ}} \qquad (1)$$

The dynamically changing charges of atoms in the QM region are derived from Mulliken population analysis[39] to describe the interactions with the atoms in the MM region, thus considering all polarization and charge-transfer fluctuations in the course of the simulation in the Coulomb term. The forces acting on the particles in the core region are evaluated as quantum mechanical plus Coulombic forces, quantum mechanical plus Coulombic forces plus non-Coulombic forces are considered in the layer region, and in the MM region the water model selected (flexible BJH[40,41]) is used for force calculation. A smoothing function $S(r)$ is applied to ensure a smooth transition between the QM and MM regions.

Structural Evaluation. Structural analyses included site−site radial distribution functions (RDFs), which are also obtainable from experimental methods.[42] In this study, the ion−O and ion−H RDFs for Fe^{2+}(aq) and Fe^{3+}(aq) ions were calculated to analyze the geometry of the first hydration shell; O−Fe^{2+}−O and O−Fe^{3+}−O angular distribution functions (ADFs) were also evaluated in combination with two additional angles, tilt (ϕ) and theta (θ), which describe the orientation of water ligands relative to the ions. These tilt and theta angles[43] are defined as the angle between the ion−O vector and the plane formed by the two O−H vectors and the angle between the ion−O vector and the sum of the two O−H vectors, respectively (see Figure 1). The coordination number distributions (CNDs) for the first and second hydration shells of Fe^{2+} and Fe^{3+} ions were also evaluated up to the first and second hydration shell minima.

Evaluation of Dynamics. The mean residence times (MRTs) τ for all of the incoming and outgoing water ligands of the second shell of the ions were calculated utilizing the direct method,[44]

---

(27) Rode, B. M.; Hofer, T. S.; Randolf, B. R.; Schwenk, C. F.; Xenides, D.; Vchirawongkwin, V. *Theor. Chem. Acc.* **2006**, *115*(2), 77.

(28) Remsungnen, T.; Rode, B. M. *Chem. Phys. Lett.* **2003**, *367*(5), 586.

(29) Remsungnen, T.; Rode, B. M. *Chem. Phys. Lett.* **2004**, *385*(5), 491.

(30) Binkley, J. S.; Pople, J. A.; Hehre, W. J. *J. Am. Chem. Soc.* **1980**, *102* (3), 939.

(31) Stevens, W. J.; Krauss, M.; Basch, H.; Jasien, P. G. *Can. J. Chem.* **1992**, *70*(2), 612.

(32) Stevens, W. J.; Basch, H.; Krauss, M. *J. Chem. Phys.* **1984**, *81*, 6026.

(33) Cundari, T. R.; Stevens, W. J. *J. Chem. Phys.* **1993**, *98*, 5555.

(34) Dunning, T. H. *J. Chem. Phys.* **1970**, *53*, 2823.

(35) Magnusson, E.; Schaefer, H. F. *J. Chem. Phys.* **1985**, *83*, 5721.

(36) Xenides, D.; Randolf, B. R.; Rode, B. M. *J. Chem. Phys.* **2005**, *122*, 4506.

(37) Pribil, A. B.; Hofer, T. S.; Vchirawongkwin, V.; Randolf, B. R.; Rode, B. M. *Chem. Phys.* **2008**, *346*(1), 182.

(38) Pribil, A. B.; Hofer, T. S.; Randolf, B. R.; Rode, B. M. *J. Comput. Chem.* **2008**, *29*(14), 2330.

(39) Mulliken, R. S. *J. Chem. Phys.* **1955**, *23*(10), 1841.

(40) Stillinger, F. H.; Rahman, A. *J. Chem. Phys.* **1978**, *68*(2), 666.

(41) Bopp, P.; Jancso, G.; Heinzinger, K. *Chem. Phys. Lett.* **1983**, *98*, 129.

(42) Allen, M. P.; Tildesley, D. J. *Computer Simulation of Liquids*; Oxford Science Publications: New York, 2003.

(43) Hofer, T. S.; Randolf, B. R.; Rode, B. M. *J. Phys. Chem. B* **2008**, *112* (37), 11726.

(44) Hofer, T. S.; Tran, H. T.; Schwenk, C. F.; Rode, B. M. *J. Comput. Chem.* **2004**, *25*(2), 211.

Figure 1. Graphical representations of tilt and theta angle schemes.

which is based on a time interval t^* required for the duration of an exchange process, i.e., the ligand's displacement from its original coordination shell at 0.0 and 0.5 ps, denoted as $\tau^{0.0}$ and $\tau^{0.5}$. 0.5 ps for the parameter t^* corresponds to the average hydrogen-bond lifetime in water[45] and is set as a lower limit for sustainable exchange. The ratio of the number of all transitions through a shell boundary, $N_{\mathrm{ex}}^{0.0}$, to the number of changes persisting for more than 0.5 ps, $N_{\mathrm{ex}}^{0.5}$, is termed R_{ex}, and it counts the number of migration attempts required to achieve one lasting exchange event.

$$R_{\mathrm{ex}} = \frac{N_{\mathrm{ex}}^{0.0}}{N_{\mathrm{ex}}^{0.5}} \qquad (2)$$

Further, their relevant dynamical properties are the stretching frequencies for ion$-$O bonds, which were determined from the velocity autocorrelation functions (VACFs) using Fourier transformation. The normal VACFs, $C(t)$, are defined by

$$C(t) = \frac{\sum_{i}^{N_t}\sum_{j}^{N} \vec{v}_j(t_i)\,\vec{v}_j(t_i+t)}{N_t N \sum_{i}^{N_t}\sum_{j}^{N} \vec{v}_j(t_i)\,\vec{v}_j(t_i)} \qquad (3)$$

where N is the number of particles, N_t is the number of origins in time, t_i, for autocorrelation of all of the velocity components of particle J, denoted by v_j. The Fourier transformation of VACFs is directly related to the vibrational spectrum, using a correlation of 2.0 ps with 2000 averaged time origins. These ion$-$O stretching frequencies and their force constants were also compared with those of other ion hydrate studies in QMCF-MD simulations.

Simulation Protocol. The simulation boxes consist of one ion (Fe^{2+}/Fe^{3+}), and 1000 water molecules with a side length of 31.10 Å, corresponding to the density of pure water measured at 298 K (0.997 g cm^{-3}), were pre-equilibrated. The Newtonian equations of motion were integrated with a time step of 0.2 fs using an Adams$-$Bashforth predictor$-$corrector algorithm, and periodic boundary conditions were applied. The temperature was controlled by the Berendsen algorithm[46] to sample a canonical (*NVT*) ensemble by coupling the system to a heat reservoir at 298 K with a coupling constant of 0.2 ps. Long-range Coulombic interactions were taken into account by the reaction field method, and the cutoff distance was set to 15.0 Å, whereas for non-Coulombic interactions, cutoff distances of 5.0 and 3.0 Å were used for O$-$H and H$-$H interactions among water molecules, respectively. The water model used in this simulation was the flexible BJH$-$CF2;[40,41] the inclusion of intramolecular parameters provides the full flexibility that is essential for smooth transitions between QM and MM regions. The initial configuration of each system was taken from geometry optimization of hexahydrated ferrous $[Fe(H_2O)_6]^{2+}$ and ferric $[Fe(H_2O)_6]^{3+}$ ions, and both simulations were performed at the unrestricted open-shell HF level of theory by employing the previously mentioned basis sets. These systems were subjected to equilibration for 4 ps, after which sampling was performed only for 8 ps. The radius of the core zone was 3.3 Å, the layer zone extended to 5.8 Å, and the smoothing region ranged from 5.6 to 5.8 Å.

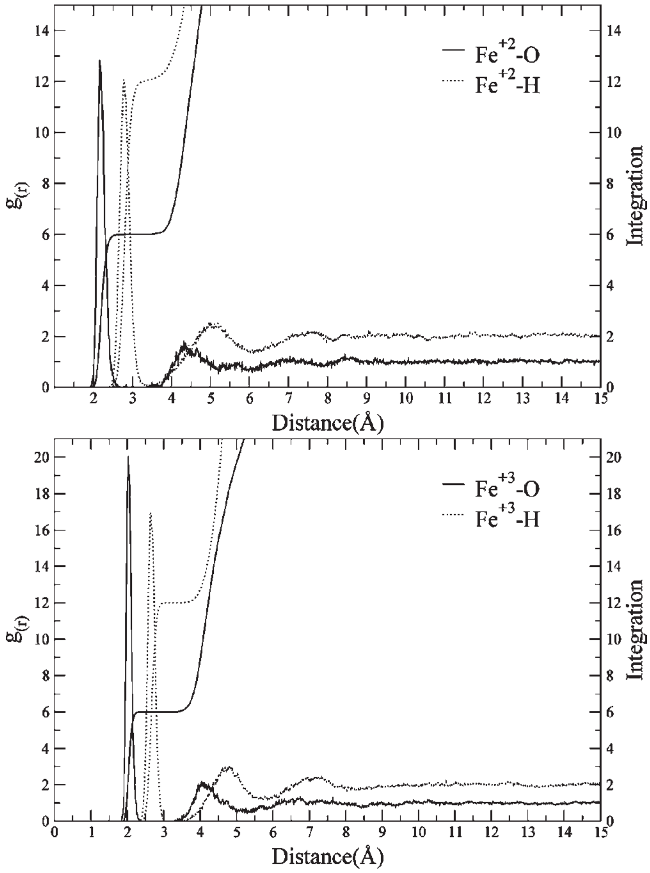

Figure 2. (a) $Fe^{2+}-O$ (solid line) and $Fe^{2+}-H$ (dotted line) and (b) $Fe^{3+}-O$ (solid line) and $Fe^{3+}-H$ (dotted line) RDFs and their running integration numbers obtained from QMCF-MD simulations.

3. Results and Discussion

Structural Properties of Hydrated Fe^{2+} and Fe^{3+} Ions. The hydration structures of Fe^{2+} and Fe^{3+} ions were primarily analyzed in terms of ion$-$O and ion$-$H RDFs, which show two distinct hydration shells with an additional weak and diffuse third hydration shell, reflecting the long-range influence of these ions on the water molecules (Figure 2a,b). The first-shell maxima at 2.15 and 2.03 Å from ion$-$O RDFs exhibit the most probable ion$-$O distance for Fe^{2+} and Fe^{3+} ions, respectively. Accordingly, the second hydration shell falls into the ranges of 3.75$-$5.25 Å and 3.5$-$5.0 Å for Fe^{2+} and Fe^{3+} ions. These structural characteristics are in good agreement with those of previous theoretical and experimental studies,[47,48] summarized in Table 3. The shape of the first-shell peak of the ion$-$O RDF of Fe^{3+}reveals a more tightly bound first shell compared to that of the Fe^{2+} ion, due to the half-width of these peaks, calculated as 0.35 and 0.25 Å, respectively. Integration of the $Fe^{n+}-O$ and $Fe^{n+}-H$ RDF plots yielded a sharp first-shell

---

[45] Rode, B. M.; Schwenk, C. F.; Hofer, T. S.; Randolf, B. R. *Coord. Chem. Rev.* **2005**, *249*(24), 2993.

[46] Berendsen, H. J. C.; Postma, J. P. M.; Gunsteren, W. F. V.; DiNola, A.; Haak, J. R. *J. Chem. Phys.* **1984**, *81*(8), 3684.

[47] D'Angelo, P.; Benfatto, M. *J. Phys. Chem. A* **2004**, *108*(20), 4505–4514.

[48] Lundberg, D.; Ullström, A. S.; DAngelo, P.; Warminska, D.; Persson, I. *Inorg. Chim. Acta* **2007**, *360*(8), 2744–2750.

Table 3. Structural Characteristics for the First Hydration Shells of the Fe^{2+} and Fe^{3+} Ion, Resulting from the Ion−O RDFs as Well as from Other Theoretical and Experimental Studies

method	ion−O distance (Å)	
	Fe^{2+}	Fe^{3+}
QMCF[a]	2.15	2.03
QMMM-MD[13]	2.10	2.02
ND[8,9]	2.12	2.01
XD, ND, EX[6]	2.10−2.28	1.99−2.05
MD(CP)[29]	2.15	2.05
MD(EP)[10]	2.11−2.27	1.98−2.11
MD(PCM)[11]	2.15	2.03
MC(PCM)[12]	2.10	1.96
EXAFS[49]	2.10	1.98
EXAFS[47]	2.12	2.01

[a] This work.

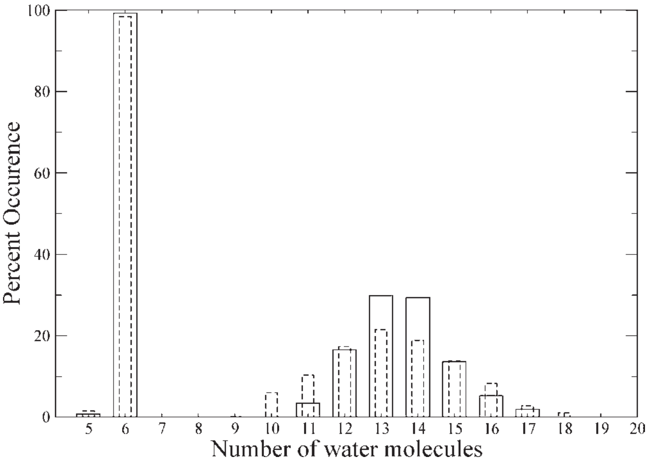

Figure 3. CNDs for the first and second shells of hydrated Fe^{2+} (dashed bars) and Fe^{3+} (solid bars) ions.

coordination number of 6 for both ions, consistent with the result obtained from the experiment.[49,47]

The CNDs for the second hydration shells of both ions were evaluated up to the boundaries of the hydration shells as obtained from the ion−O RDFs (cf. Figure 3). The CND plots show the six water ligands of the first hydration shell. The second hydration shell of Fe^{2+} contains in average of 13 water molecules, in a range from 9 to 18. For the Fe^{3+} ion, the second hydration shell shows a CND in the range of 11−17, with maxima near 13 and 14, corresponding to an average coordination number of 13.6.

The geometry of the first hydration shell is further illustrated by ADFs for Fe^{2+} and Fe^{3+} ions, also evaluated from the QMCF-MD simulations and shown in Figure 4. Two peaks are found in each O−ion−O ADF plot at 90° and 170°, proving an octahedral configuration of the $[Fe(H_2O)_6]^{2+}$ and $[Fe(H_2O)_6]^{3+}$ complexes.

The alignment of coordinating water molecules toward the Fe^{2+} and Fe^{3+} ions and their orientational freedom relative to these ions were explored by means of tilt (ϕ) and theta (θ) angle distributions as defined in the Methods section. The tilt angle distribution of the ions indicates that the water dipoles are not oriented perfectly along the ion−O axis, from which it deviates by ~16−18°. The theta angle distribution describes the orientational freedom of the water molecules within the first hydration shell, exhibiting a maximum at ~40° tailing toward ~140° for the Fe^{2+} ion and 50° and 180° for the Fe^{3+} ion, respectively. Both tilt and theta angles prove a considerable deviation from an idealized octahedral complex.

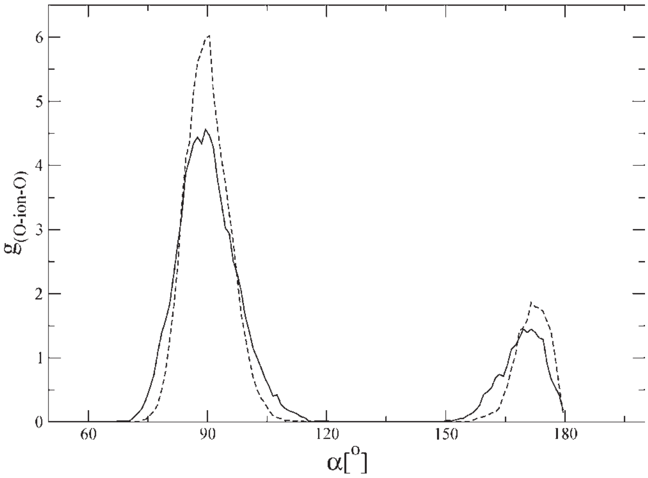

Figure 4. O−ion−O ADF for hydrated Fe^{2+} (solid line) and Fe^{3+} (dashed line).

Dynamics. Ligand-exchange reactions were not observed between the first and second hydration shells, visible from the zero regions in the g_{ion-O} (and g_{ion-H}) plots between the first and second shells of both ions. Experimental MRTs determined by NMR spectroscopy for the first hydration shell of the Fe^{2+} ion as 3×10^{-7} s[50] and in the range of 5×10^{-5} [51] to 6×10^{-3} s[52] for Fe^{3+} show why in our simulation time of 8 ps no exchange could be expected. The ligands of the second hydration shell are involved in multiple exchanges with the bulk, as depicted in the ion−O distance plots for the Fe^{2+} and Fe^{3+} ions in an aqueous solution shown in Figure 5a,b, with some water molecules highlighted: a water molecule constantly present in the stable first hydration shell, a water molecule migrating from the second hydration shell to the bulk, and a water molecule entering the second hydration shell from the bulk. Figure 5 also illustrates that the water molecules coordinated to Fe^{2+} are fluctuating to longer distances compared to those bound to the Fe^{3+} ion, with its more tightly bound first hydration shell.

Ligand MRTs, τ, for the second hydration shells of the Fe^{2+} and Fe^{3+} ions have been compared with the MRT value of pure water (Table 4). With 2.4 and 3.1 ps, respectively, they are still lower than the estimated value in the range of 10^{-10}−10^{-11} s for the aqueous Fe^{3+} ion.[9] It should be mentioned, however, that any estimation not based on a femtosecond laser probe experiment is not able to produce reliable data for rates above 10^{10} s. On the other hand, compared with the value of 1.3 ps for pure water, both ions display a structure-forming ability up to the second hydration shell. To have deeper insight into the dynamics of the second hydration shell of Fe^{2+} and Fe^{3+}, the data for exchange processes were compared,

---

(49) Brunschwig, B. S.; Creutz, C.; Macartney, D. H.; Sham, T. K.; Sutin, N. *Faraday Discuss. Chem. Soc.* **1982**, *74*, 113.

(50) Swift, T. J.; Connick, R. E. *J. Chem. Phys.* **1962**, *37*, 307.

(51) Fiat, D.; Connick, R. E. *J. Am. Chem. Soc.* **1968**, *90*(3), 608.

(52) Grant, M.; Jordan, R. B. *Inorg. Chem.* **1981**, *20*(1), 55.

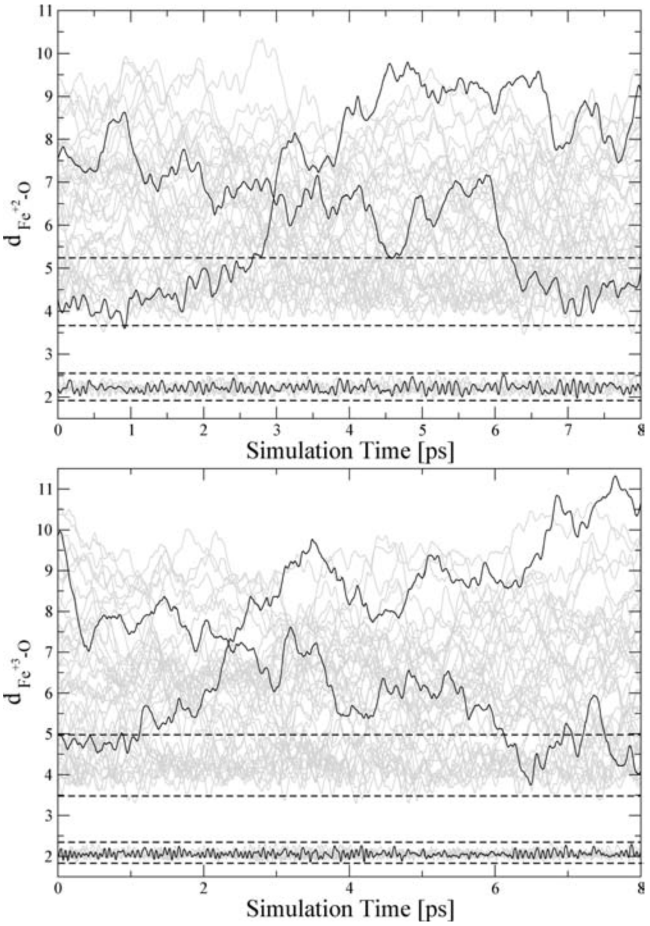

Figure 5. Plots of distances between (a) Fe^{2+} and water O atoms and (b) Fe^{3+} and water O atoms of the first and second hydration shells.

Table 4. Characteristic Data for the Solvent Dynamics for Second-Shell Water Ligands of Fe^{2+} and Fe^{3+} Ions and Pure Water[a]

ion (method)	CN	$N_{ex}^{0.5}$	$N_{ex}^{0.0}$	$\tau_{0.5}$ (ps)	$\tau_{0.0}$ (ps)	R_{ex}
Fe^{2+} (QMCF-MD)	13.3	46	305	2.4	0.34	6.6
Fe^{3+}(QMCF-MD)	13.6	35	254	3.1	0.42	7.2
Fe^{2+} (QM/MM MD)[44]	14.4	31	359	5.4	0.6	11.6
Fe^{3+} (QM/MM MD)[44]	14.0	6	157	19.8	0.8	26.2
H_2O[56]	4.1	20	131	1.3	0.19	6.5
H_2O[44]	4.1	24	269	1.7	0.2	11.2

[a] N_{ex} is the number of exchange events, R_{ex} is the number of attempts needed to produce one lasting exchange, and CN is the average coordination number.

Table 5. Ion−O Stretching Frequencies and Corresponding Force Constants of Hydrated Fe^{2+} and Fe^{3+} Ions

ion	method	Q_{ion-O} (cm^{-1})	F_{ion-O} (N m^{-1})
Fe^{2+}	QMCF-MD	357	93
Fe^{3+}	QMCF-MD	513	193
Pb^{2+}	QMCF-MD[54]	196	33.6
Zn^{2+}	QM/MM MD[53]	310	73
Al^{3+}	QMCF-MD[43]	560	185
Fe^{2+}	Raman scattering[57,58]	380	106
Fe^{3+}	Raman scattering[59]	520	198

and it was observed that 46 exchange processes lasted longer than 0.5 ps for the Fe^{2+} ion, whereas for Fe^{3+}, only 35 exchange events were observed, verifying the more stable second hydration shell of Fe^{3+} compared to Fe^{2+}. Table 4 also includes data for the second-shell dynamics of ions, obtained from a previous QM/MM MD simulation[13] in which only one hydration shell was treated quantum mechanically. The coordination numbers of the second hydration shell are similar in both types of simulations, but the dynamic characteristics show strong differences. The apparently too high MRT values resulting from the conventional one-shell QM/MM MD simulation are partly an "artifact" linked to the assignment of fixed charges to the QM atoms while using paired three-body potentials in this scheme, partly a problem of describing hydrogen bonds between the first and second shells chemically. The inclusion of the second hydration shell in the QM region in the QMCF formalism offers significant improvements for the description of these hydrogen bonds, and the improved embedding scheme enhances these improvements.

The fluctuation in the effective charges of aqueous Fe^{2+} and Fe^{3+} ions was also monitored by performing Mulliken population analysis during the course of the whole simulation, and these charges are in the range of 1.25−1.45, with an average value of 1.36 for Fe^{2+}, and the average charge for Fe^{3+} was 1.85, ranging between 1.70 and 1.95. The inclusion of more realistic fluctuating point charges for the two hydration shells in QMCF-MD compared to QM/MM MD results in the improved evaluation of Coulombic forces between the first and second hydration layers. The fixed point charges for the water molecules in the previous methodology experience a strong electrostatic attraction between hydration shells, resulting in a strong electrostatic attraction between the first and second hydration layers.

Besides the evaluation of the MRT values, the dynamic behavior of the Fe^{2+} and Fe^{3+} ions was also characterized by evaluation of the ion−O stretching frequencies, which were compared with those obtained from experiments. To determine the relative strength of ion−O bonds in hydrated Fe^{2+} and Fe^{3+} ions, they were also compared with the ion−O frequencies of other divalent and trivalent ions (cf. Table 5). The ion−O stretching frequencies from the QMCF-MD simulations in water are in very good agreement with the experimental values. The frequency of the Fe^{2+}−O stretching mode corresponds to a force constant of 93 N m^{-1} (exptl 106 N m^{-1}), which is higher than the values for other divalent ions such as Zn^{2+} [53] and Pb^{2+}.[54] The stretching frequency for the Fe^{3+}−O bond corresponds to a force constant of 193 N m^{-1} (exptl 198 N m^{-1}), which is higher than the force constant obtained for hydrated Al^{3+} (185 N m^{-1}),[43] classifying the Fe^{3+}−O bond stronger than the Al^{3+}−O bond, which is due to the contribution of covalent interaction along with electrostatic interaction. These spectroscopic data also seem to validate the accuracy level of the QMCF-MD simulation technique.

The average stabilization energies (ΔE_{stab}) of hydrated Fe^{2+} and Fe^{3+} ions from QMCF-MD simulations are also compared with the experimental enthalpies of hydration (ΔH_{hyd}^{exp}) for both ions. The experimental molar

---

(53) Fatmi, M. Q.; Hofer, T. S.; Randolf, B. R.; Rode, B. M. *J. Chem. Phys.* **2005**, *123*, 4514.

(54) Bhattacharjee, A.; Hofer, T. S.; Pribil, A. B.; Randolf, B. R.; Lim, L. H. V.; Lichtenberger, A. F.; Rode, B. M. *J. Phys. Chem. B* **2009**, *113*(39), 13007.

enthalpies of hydration were computed, based on the TATB approximation, as −471 and −1066 kcal mol^{-1} for Fe^{2+} and Fe^{3+} ions,[55] respectively. The average hydration energies from the simulations are −512 and −1115 kcal mol^{-1} for these ions, in good agreement with the experimental values.

4. Conclusion

The description of the hydration structures of the Fe^{2+} and Fe^{3+} ions is significantly improved by the ab initio QMCF-MD formalism treating two hydration layers quantum mechanically, compared to conventional QM/MM approaches including the ion and only one hydration shell. The resulting ion−O distances are now within the limits of the experimental values, and other data such as force constants, ligand MRTs, and exchange rates could also be improved; e.g., the ion−O stretching frequencies closely agree with the experimental results. The reasons for the improvements in the new simulation methodology are seen in the significantly larger QM region, which includes all binding between the first and second shells in the quantum mechanical force calculations, and in the use of the more realistic fluctuating atomic charges of all species in the QM region and a better embedding scheme introducing the MM charges as a perturbation in the core Hamiltonian of the whole QM region. The results for the structure and dynamics of divalent and trivalent iron ions in the dilute aqueous solution presented here are considered, therefore, as a major advance in the characterization of these ions, chemically and biologically important in manifold ways.

Acknowledgment. Financial support for this work by the Austrian Science Foundation (FWF) and an Austrian Technology grant (Grant BMWF/RFTE) for S.T.M. are gratefully acknowledged.

---

(55) Marcus, Y. *Ion Solvation*; Wiley: New York, 1985.

(56) Randolf, B. R.; Hofer, T. S.; Rode, B. M. Unpublished results.

(57) Jenkins, J.; Lewis, J. *Spectrochim. Acta* **1981**, *37*(1), 47.

(58) Halley, J. W.; Hautman, J. *Ber. Bunsen. Phys. Chem.* **1987**, *91*, 491.

(59) Best, S. P.; Armstrong, R. S.; Beattie, J. K. *Inorg. Chem.* **1980**, *19*(7), 1958.